

# Flux qubit with a large loop size and tunable Josephson junctions\*

Deng Hui(邓辉), Yu Hai-Feng(于海峰), Xue Guang-Ming(薛光明),  
Tian Ye(田野), Ren Jian-Kun(任建坤), Wu Yu-Lin(吴玉林),  
Huang Ke-Qiang(黄克强), Zhao Shi-Ping(赵士平), and Zheng Dong-Ning(郑东宁)<sup>†</sup>

*Beijing National Laboratory for Condensed Matter Physics, Institute of Physics,  
Chinese Academy of Sciences, Beijing 100190, China*

(Received 16 December 2011; revised manuscript received 29 December 2011)

We present the design of a superconducting flux qubit with a large loop inductance. The large loop inductance is desirable for coupling between qubits. The loop is configured into a gradiometer form that could reduce the interference from environmental magnetic noise. A combined Josephson junction, i.e., a DC-SQUID is used to replace the small Josephson junction in the usual 3-JJ (Josephson junction) flux qubit, leading to a tunable energy gap by using an independent external flux line. We perform numerical calculations to investigate the dependence of the energy gap on qubit parameters such as junction capacitance, critical current, loop inductance, and the ratio of junction energy between small and large junctions in the flux qubit. We suggest a range of values for the parameters.

**Keywords:** flux qubit, four Josephson junctions, tunable energy gap

**PACS:** 03.67.Lx, 85.25.Cp, 85.25.Dq

**DOI:** 10.1088/1674-1056/21/4/040307

## 1. Introduction

Superconducting nano-circuits consisting of Josephson junctions (JJs) are promising candidates for qubits, the building block of quantum computers. According to the ratio of Josephson coupling energy  $E_J = \hbar I_c / 2e$  to charge energy  $E_C = 2e^2 / C$ , the superconducting qubits may be divided into three categories, i.e. charge qubits, flux qubits, and phase qubits.<sup>[1–8]</sup> There are advantages and disadvantages for each type of the superconducting qubits. For example, the charge qubits are sensitive to the charge fluctuations of background while the phase qubits may be more influenced by flux noise. Great effort has been made to study the superconducting qubits in the past decade and tremendous progress has been achieved. One of the key challenges to the superconducting qubits (as well as to other solid state qubits) is the relatively short decoherence time. So far, the flux qubit has shown the longest decoherence time among all three types. For example, Bylander *et al.*<sup>[9]</sup> have shown that a flux qubit with decoherence time goes up to 12  $\mu$ s.

Almost all the flux qubits studied are based on

the design proposed by Mooij and Orlando *et al.*<sup>[10,11]</sup> In this design, the qubits consist of 3 JJs or 4 JJs with small loop inductance.<sup>[12]</sup> An advantage of this design is that the flux noise which is proportional to the loop size<sup>[13]</sup> can be minimized significantly. So far, this type of flux qubit has achieved considerable progress and, in particular, demonstrated a long quantum coherence time. However, there are several drawbacks associated with the design. The major problem results from the small loop size that brings much difficulty in inter-qubit coupling and, hence, hinders the scalability. Therefore, in order to balance the coherence time and inter-qubit coupling, it would be desirable to find a range of qubit loop sizes to compromise these two conflict issues within the experimental tolerance.

Another problem is the barrier height that is proportional to the energy gap between the ground state and the first excited state and could not be adjusted once the qubit has been fabricated in the original design of Mooij. This leads to inconvenience for choosing the circuitry parameters and limits the application of the flux qubits in more advanced measurement methods such as freeze state technique.<sup>[14]</sup> This problem has been addressed by replacing the small JJ in

\*Project supported by the National Basic Research Program of China (Grant Nos. 2011CBA00106 and 2009CB929102) and the National Natural Science Foundation of China (Grant Nos. 11104340, 11161130519, and 10974243).

<sup>†</sup>Corresponding author. E-mail: dzheng@aphy.iphy.ac.cn

© 2012 Chinese Physical Society and IOP Publishing Ltd

<http://iopscience.iop.org/cpb> <http://cpb.iphy.ac.cn>

the flux qubit with a combined JJ (CJJ), i.e. a DC SQUID, of which the critical current (and, thus, the barrier height) can be changed by the application of local external fluxes.<sup>[12]</sup>

Additionally, almost all of the flux qubit samples studied in the literature are based on aluminium Josephson junctions fabricated by using the shadow evaporation technique. Although this fabrication process is simple and can obtain sub-micron small size JJs easily, it cannot prepare complex circuits from a long-term point of view. Today, the fabrication of complex JJ circuits using the tri-layer technology<sup>[15]</sup> is the standard approach in the field of superconducting electronics. Therefore, for scalable qubit circuits that should consist of a large number of qubit cells, niobium or aluminum JJs prepared using the tri-layer technology should also be considered. In general, the size of a JJ made by using tri-layer technology cannot be very small (the size is usually larger than 0.2  $\mu\text{m}$ ) as in the case of junctions made by the shadow evaporation method. As a result, the selections of qubit parameter could be quite different for these two fabrication methods. Considering the large loop inductance mentioned above, the potential of the flux qubit becomes a three-dimensional (3D) problem that is much different from 2D one. Thus, a detailed and systemic study of the qubit parameters based on tri-layer technology is of considerable importance. In this paper, we present a systematic study of the qubit parameters of a flux qubit with large loop size and a relatively large junction size that can be realized using tri-layer fabrication technology. We also replace the third small junction of the 3-JJ flux qubit design with a compound JJ as indicated in Ref. [12]. In this way, the energy gap between the ground state and the first excited state can be well controlled by an independent flux bias line. By calculating the energy levels, we discuss the dependence of energy gap  $\Delta$  on the capacitance  $C$ , the critical current  $I_c$  of junctions, the qubit loop inductance  $L$ , and the normalized critical current of CJJ  $\alpha_I = 2I_{CJJ}/(I_{01} + I_{02})$ . The results are instructive for designing this type of flux qubit.

## 2. Qubit design and its Hamiltonian

A flux qubit is usually made of a superconducting loop interrupted by one or three JJs. Although both designs function similarly, the latter is more popular than the first one (rf-SQUID type). To the best

of our knowledge, no macroscopic quantum coherence phenomenon had been demonstrated in a single JJ flux qubit up to now. Apart from the reason that the large loop size leads it to be vulnerable to dephasing by magnetic fluctuations of the environment, a more important reason is that the separation between the two potential double wells of one JJ model is much larger than that of 3-JJ model. This difference means that the barrier must be sufficiently low so that the tunneling effect between the two wells is of significance, thereby being able to observe the coherence between qubit states. However, a very low barrier would also mean that a phase particle can easily hop from one well to another by thermal activation, resulting in dephasing. So the design of a one JJ model has been hardly investigated and the 3-JJ model has become more popular.

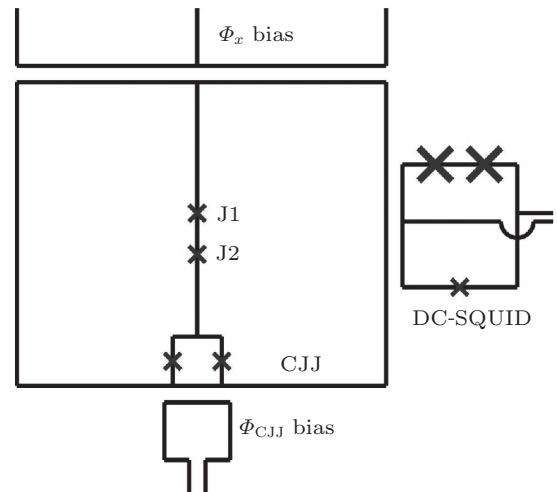


**Fig. 1.** Schematic diagram of a 4-JJ flux qubit. The junctions, denoted by the thick cross, sit in the middle arm of qubit. The fluxes through the qubit and the CJJ are biased with  $\Phi_x$  line and  $\Phi_{CJJ}$  line, respectively. An asymmetric DC SQUID is used to readout the qubit signal. The four junctions in the qubit loop are designed to have the same sizes. The parameter relations between the CJJ and the middle arm junctions are  $\alpha_c = 2$  for capacitance and  $\alpha_I = 0 \sim 2$  for critical currents depending on the  $\Phi_{CJJ}$  bias.

The schematic diagram of the flux qubit we considered is shown in Fig. 1. The superconducting loop is designed in a gradiometer structure to reduce the influence of environmental flux noise. The four junctions with the same sizes are denoted by a thick crossed line. Junction 1 (J1) and junction 2 (J2) sit on the middle arm, and the other two constitutes a DC SQUID configuration. The critical current of the CJJ, which determines the energy gap  $\Delta$ , can be modulated by an independent flux bias line  $\Phi_{CJJ}$ . It

is worthwhile to point out that when the junction size is small, it is easier to make the 4 JJs into the same size by using tri-layer technology. The detuning  $\varepsilon$  of the qubit is controlled by another independent flux bias line  $\Phi_x$ . The qubit energy difference is then given by  $E_{01} = \sqrt{\Delta^2(\alpha_I) + \varepsilon^2(\Phi_x)}$ <sup>[16]</sup> where  $\alpha_I = 2I_{CJJ}/(I_{01} + I_{02})$ , and  $I_{0i}$  ( $i = 1, 2$ ) are the critical currents of J1 and J2. The cross talk between  $\Phi_x$  and the CJJ as well as the cross talk between  $\Phi_{CJJ}$  and the qubit loop can be neglected due to the symmetric design. The qubit signal is readout by an asymmetric DC SQUID. The loop inductance is about 100 pH–200 pH, which is much larger than the typical value ( $\sim 10$  pH) of most designs reported in the literature.

The main feature of the 4-JJ design is that although the relative capacitance (or, junction area size) parameter  $\alpha_c = 2C_{CJJ}/(C_1 + C_2)$ , which is determined by the fabrication, cannot change, we can adjust the CJJ critical current  $\alpha_I$  by varying  $\Phi_{CJJ}$ . While in the case of 3-JJ we have  $\alpha_I = \alpha_c$  and cannot change  $\alpha_I$  after fabrication. To obtain the maximal controllable range of  $\alpha_I$ , also the reasonable qubit gap (see Section 3), one choice is to reduce the four junctions to the smallest size allowed by the tri-layer fabrication technology. As a result, we have  $\alpha_c \equiv 2$  and  $\alpha_I$  can change from 0 to 2.

In order to calculate the energy levels of the qubit, one needs to know the potential energy first. The method is similar to that by Robertson *et al.*<sup>[17]</sup> However in their discussion a 3-JJ flux qubit was used, therefore, the junction parameters were determined completely by fabrication. In contrast, in the 4-JJ design discussed here we can change the critical current and keep the capacitance fixed. Because the critical current determines the potential energy and the capacitance determines the kinetic energy the 4-JJ design provides additional flexibility in measurements.

The potential energy consists of two parts that represent the contributions of the Josephson junctions and the superconducting loop, respectively. Naturally, the potential energy can be expressed as a function of the loop inductance and the phase difference cross the JJs in the qubit. Thus,

$$U = U_1 + U_J, \quad (1)$$

$$U_1 = LJ^2/2, \quad (2)$$

$$U_J = \frac{\Phi_0}{2\pi} [I_{01}(1 - \cos \gamma_1) + I_{02}(1 - \cos \gamma_2) + I_{CJJ}(1 - \cos \gamma_{CJJ})]. \quad (3)$$

However, by considering the flux quantization, we have

$$\gamma_1 + \gamma_2 + \gamma_{CJJ} = \phi_x + \frac{2\pi LJ}{\Phi_0}, \quad \phi_x = 2\pi \frac{\Phi_x}{\Phi_0}, \quad (4)$$

Here  $J$  is the circulating current through the central axis of the qubit,  $\Phi_0 = h/2e$  is the flux quanta,  $h$  is the Planck constant,  $I_{0i}$  and  $\gamma_i$  ( $i = 1, 2$ ) are the critical currents of phase differences of J1 and J2,  $I_{CJJ}$  and  $\gamma_{CJJ}$  are the effective critical currents of phase differences of the CJJs, and  $L$  is the geometrical inductance. We also have changed the applied flux  $\Phi_x$  into a quantity of phase unit  $\phi_x$ .

We then define a dimensionless inductance parameter  $\beta$ , and  $\kappa$ , due to the asymmetry between J1 and J2, as

$$\beta = \frac{2\pi L}{\Phi_0} \left( \frac{1}{I_{01}} + \frac{1}{I_{02}} + \frac{1}{I_{CJJ}} \right)^{-1} \quad \text{and} \\ \kappa = \frac{I_{01} - I_{02}}{I_{01} + I_{02}}. \quad (5)$$

In order to see the potential energy more clearly, we introduce the total phase variables  $\gamma_a$ ,  $\gamma_s$ , and  $\gamma_t$  to construct new coordinate axis along the zero inductive energy plane as follows:<sup>[17]</sup>

$$\gamma_a = (\gamma_1 - \gamma_2)/2, \quad (6)$$

$$\gamma_s = \frac{1}{2(1 + 2\alpha_I)} [2\alpha_I(\gamma_{CJJ} - \phi_x) - \gamma_1 - \gamma_2], \quad (7)$$

$$\gamma_t = \alpha_I(\phi_x - \gamma_1 - \gamma_2 - \gamma_{CJJ})/(1 + 2\alpha_I). \quad (8)$$

Then, Eqs. (2) and (3) can be rewritten as

$$U_1 = E_J \frac{(1 + 2\alpha_I)^2 (1 - \kappa^2)}{2\alpha_I \beta (1 + 2\alpha_I - \kappa^2)} \gamma_t^2, \quad (9)$$

$$U_J = -E_J [(1 + \kappa) \cos(\gamma_a - \gamma_s - \gamma_t) + (1 - \kappa) \cos(\gamma_a + \gamma_s + \gamma_t) + \alpha_I \cos(2\gamma_s + \phi_x - \gamma_t/\alpha_I)], \quad (10)$$

where  $E_J = (I_{01} + I_{02})\Phi_0/4\pi$ .

In Figs. 2(a) and 2(b) we show the potential energies from Eq. (1) in a 3D fashion for both large loop inductance ( $\beta = 0.3$ ) and very small loop inductance ( $\beta = 0.001$ ), respectively. We can see from Fig. 2(a) that large loop inductance bends the potential wells and increases the effective tunneling path. In contrast, for small inductance as shown in Fig. 2(b), the path is confined within the constant  $\gamma_t = 0$  plane, so the 3D problem becomes a 2D one as if the qubit loop inductance can be ignored.

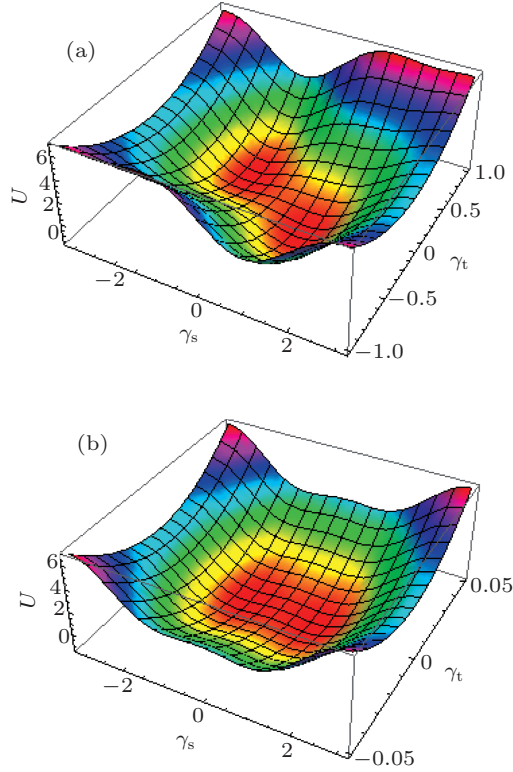


**Fig. 2.** (colour online) The 3D qubit potentials for  $\alpha_I = 0.8$ ,  $\beta = 0.3$ ,  $\phi_x = \pi$ ; the tunneling path is bent from the contribution of large loop inductance (a), and for  $\alpha_I = 0.8$ ,  $\beta = 0.001$ ,  $\phi_x = \pi$ , the tunneling path is confined in  $\gamma_t = 0$  plane (b), so the 3D potential reduces to a 2D one.

The kinetic energy of the system is

$$T_{\text{qubit}} = \frac{\Phi_0^2}{8\pi^2} \left[ C_1 \dot{\gamma}_1^2 + C_2 \dot{\gamma}_2^2 + C_{\text{CJJ}} \dot{\gamma}_{\text{CJJ}}^2 \right], \quad (11)$$

where  $C_i$  ( $i = 1, 2, \text{CJJ}$ ) are the capacitances of J1, J2, and CJJ. For simplicity, we have ignored the influence of stray capacitance.<sup>[17]</sup> In our case, because all junctions are of the same size, we have  $C_1 = C_2 = C_{\text{CJJ}}/2 = C$ , and  $I_{01} = I_{02} = I_{\text{CJJ}}/2 = I_c$ .

The Hamiltonian of this type of flux qubit is,

$$H = \mathbf{P} \cdot \mathbf{M}^{-1} \cdot \mathbf{P}/2 + U, \quad (12)$$

where the first term is just  $T_{\text{qubit}}$  in Eq. (11).

To solve the eigenvalue problem of the qubit Hamiltonian, we expand the wave function by the product of plane-wave solutions and harmonic eigenfunctions, compute each of the matrix elements of Hamiltonian and diagonalize this matrix.<sup>[17]</sup> The diagonal elements are just the eigenvalues. Figure 3 shows the calculated results of the energy levels at typical parameters that can be achieved in the tri-layer technology ( $I_c = 320$  nA,  $C = 7.2$  fF,  $L = 100$  pH, and  $\alpha_I = 0.62$ ). We can see that at the degeneracy point

( $\phi_x = \pi$ ), the ground state and the first excited state energy levels are anti-crossing and well separated from other higher levels. The two qubit states are given by  $|0\rangle = (|\uparrow\rangle + |\downarrow\rangle)/2$  and  $|1\rangle = (|\uparrow\rangle - |\downarrow\rangle)/2$ , where  $|\uparrow\rangle$  and  $|\downarrow\rangle$  denote the clockwise and the counterclockwise states.

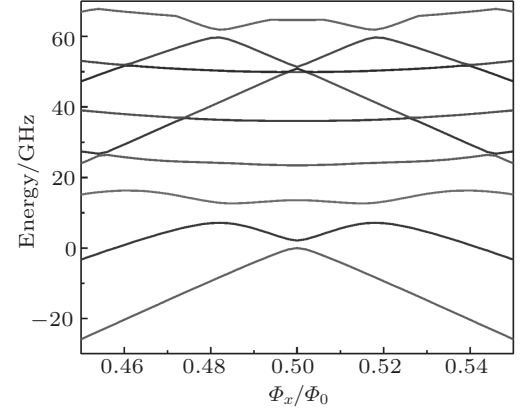


**Fig. 3.** Energy levels of 4JJs flux qubit versus reduced magnetic flux  $\Phi_x/\Phi_0$ . The diagram shows only nine levels, of which the two lowest levels used for the qubit. Parameters are chosen to be  $C = 7.2$  fF,  $I_c = 0.32$   $\mu\text{A}$ ,  $L = 100$  pH, and  $\alpha_I = 0.62$ .

### 3. Qubit parameters based on the tri-layer fabrication process

Several factors should be taken into account when a flux qubit is designed. Firstly, on the one hand, because the flux noise is proportional to the qubit loop size, the loop size should not be too large. On the other hand, in order to have enough coupling strength between one qubit and others, which is crucial for a scalable quantum circuits, the loop size should not be too small. Thus, the size about 50  $\mu\text{m}$ –80  $\mu\text{m}$  is chosen. The inductance is about 100 pH–200 pH as calculated by using the Fast-Henry program.<sup>[18]</sup> Secondly, the energy gap  $\Delta$  between the ground and the first excited states must be considerably larger than the thermal noise energy  $k_B T$ , where  $T$  is noise temperature which is usually about 30 mK ( $\sim 0.6$  GHz). Otherwise, the qubit cannot be initialized to the ground state. Thirdly, the energy gap between the first excited state and the higher excited state must be larger than the energy gap to avoid multi-transitions in an alternating current (AC) field. Bearing these three points in mind, we discuss the qubit parameters specially.

**Capacitance** Capacitance is, arguably, the most important parameter for the design of this type of flux

qubit. Figure 4(a) shows the exponential decay dependence of energy gap  $\Delta$  on junction capacitance value, which is scaled mainly with the junction area. A typical value of the geometrical capacitance for Nb/Al-AlO<sub>x</sub>/Nb and Al/AlO<sub>x</sub>/Al JJ is about 45 fF/ $\mu\text{m}^2$  for  $J_c < 1000 \text{ A/cm}^2$ . Because of the complexity in the tri-layer process, it is difficult to make a junction size of less than 0.2  $\mu\text{m}$  as in the double-angle shadow evaporation process. To achieve a large energy gap, the size of the junction should be as small as possible. For practical fabrication, we suggest that the junction area size is in a range of 0.3  $\mu\text{m}$ –0.5  $\mu\text{m}$  that corresponds to the capacitance value in a range of 4.5 fF–11 fF.

**Loop inductance** From Fig. 4(b) we find that the energy gap has a linear dependence on loop inductance and the drop varies slightly with loop inductance increasing. Although the energy gap  $\Delta$  has a weak dependence on loop inductance, the balance between flux noise and the coupling strength with other qubits leads to a reasonable value that is between 100 pH to 200 pH.

**Critical current** The critical current density  $J_c$  can be easily and accurately controlled from 40 A/cm<sup>2</sup>

to 2000 A/cm<sup>2</sup> by the oxidation time and oxygen pressure. In Fig. 4(c), we plot the energy gap  $\Delta$  as a function of the critical current of JJ. We find that  $\Delta$  decreases with  $I_c$  increasing, which indicates that  $I_c$  should not be too large to reduce the value of  $\Delta$ . However, the large  $I_c$  value favours the detection of the flux qubit state by using a DC-SQUID. Furthermore, for a flux qubit, the ratio between Josephson energy and charge energy  $E_J/E_C$  is around 100, thus the value of  $I_c$  cannot be too small. Within an acceptable region, we chose the critical current value to be about 200 nA–400 nA for the CJJ. This means that the  $I_c$  of each junction of CJJ is about 100 nA–200 nA. Of course,  $I_c$  can be adjusted by an external flux provided by  $\Phi_{\text{CJJ}}$ .

$\alpha_I$ : compared with the above parameters,  $\alpha_I$  is a free parameter because it can be tuned by magnetic flux through CJJ loop  $\Phi_{\text{CJJ}}$ . Figure 4(d) shows that  $\Delta$  decreases with  $\alpha_I$  increasing and has a weak linear dependence on it when  $\alpha_I$  is smaller than 0.6. Besides, one should keep in mind that  $\alpha_I < 1$  must be fulfilled. Otherwise, the intra-cell tunneling will be suppressed by inter-cell tunneling from different unit cells.<sup>[11]</sup>

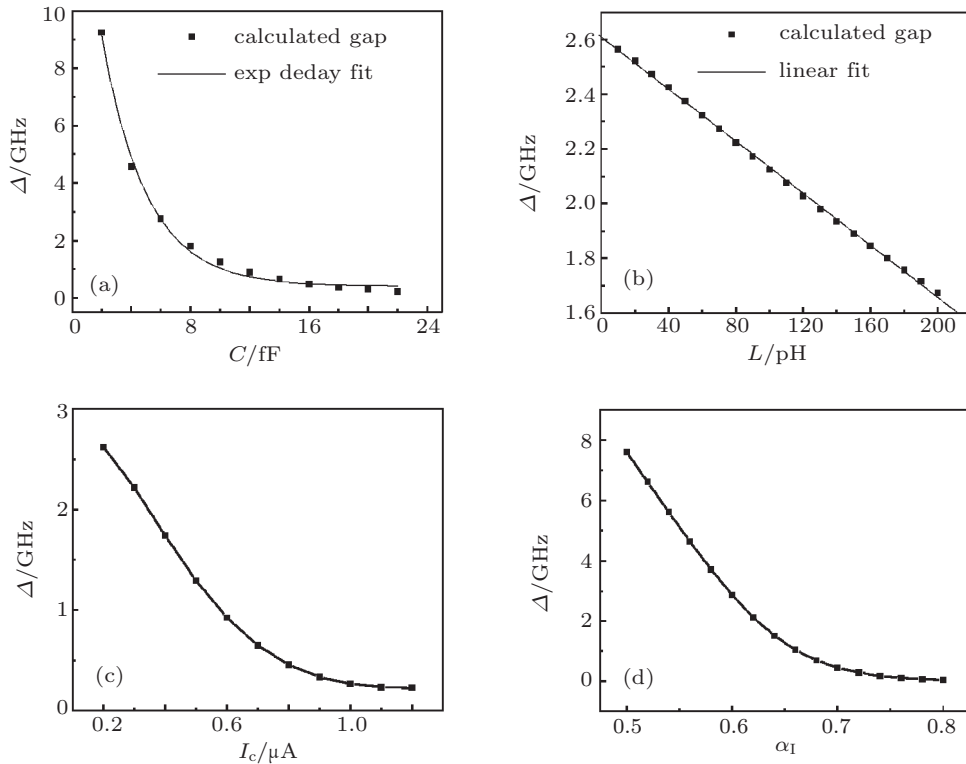


**Fig. 4.** Values of energy gap  $\Delta$  versus (a) capacitance, with other parameters being  $L = 100 \text{ pH}$ ,  $I_c = 0.32 \text{ }\mu\text{A}$ , and  $\alpha_I = 0.62$ , and the data fitted by exponential decay function; (b) loop inductance, with other parameters being  $C = 7.2 \text{ fF}$ ,  $I_c = 0.32 \text{ }\mu\text{A}$ ,  $\alpha_I = 0.62$ , and the curve shows a linear dependence; (c) critical current of  $I_c$  at  $C = 7.2 \text{ fF}$ ,  $L = 100 \text{ pH}$ ,  $\alpha_I = 0.62$ ; and (d)  $\alpha_I$ , at  $C = 7.2 \text{ fF}$ ,  $L = 100 \text{ pH}$ ,  $I_c = 0.32 \text{ }\mu\text{A}$ .

Here, it should be emphasized that the available parameter ranges of this type of qubit, especially the capacitance, are not wide because of the small energy gap. Considering characters of tri-layer technology, we suggest the following parameters: junction area size between 0.3  $\mu\text{m}$  and 0.5  $\mu\text{m}$ , corresponding capacitance between 4.5 fF and 11 fF, the loop inductance between 100 pH and 200 pH, and critical current between 100 nA–200 nA for each junction.

## 4. Conclusion

In the present paper, we present a design of a superconducting flux qubit consisting of 4 JJs with a large loop inductance. Two of the four JJs form a combined JJ, namely a DC SQUID, so that the energy gap between the ground state and the first excited state can be tuned by an independent flux bias line. The large loop is formed in a gradiometer structure that reduces the influence of environmental flux noise and the large inductance is useful for coupling between flux qubits. Through solving the eigenvalues of the qubit Hamiltonian, we discuss the qubit parameters based on the trilayer technology. The results show that the large loop inductance has a weak influence on energy gap, while the junction capacitance and the critical current need to be optimized to obtain an appropriate energy gap. We present a range of values for the parameters.

## Acknowledgement

We are grateful to Deng Xiao-Di for helpful discussion about developing the program.

## References

- [1] You J Q and Nori F 2005 *Phys. Today* **58** 42
- [2] Li Z X, Zou J, Cai J F and Shao B 2006 *Acta Phys. Sin.* **55** 1580 (in Chinese)
- [3] Cao W H, Yu H F, Tian Y, Yu H W, Ren Y F, Chen G H and Zhao S P 2009 *Chin. Phys. B* **18** 5044
- [4] Wu S H, Hu M L, Li J and Xi X Q 2011 *Acta Phys. Sin.* **60** 010302 (in Chinese)
- [5] Liang B L, Wang J S, Meng X G and Su J 2010 *Chin. Phys. B* **19** 010315
- [6] Ji Y H, Lai H F, Cai S H and Wang Z S 2010 *Chin. Phys. B* **19** 030310
- [7] Jiang W, Yu Y and Wei L F 2011 *Chin. Phys. B* **20** 080307
- [8] Cong S H, Wang Y W, Sun G Z, Chen J, Yu Y and Wu P H 2011 *Chin. Phys. B* **20** 050316
- [9] Bylander J, Gustavsson S, Yan F, Yoshihara F, Harrabi K, Fitch G, Cory D G, Nakamura Y, Tsai J S and Oliver W D 2011 *Nature Phys.* **7** 565
- [10] Mooij J E, Orlando T P, Levitov L, Tian L, van der Wal C H and Lloyd S 1999 *Science* **285** 1036
- [11] Orlando T P, Mooij J E, Tian L, van der Wal C H, Levitov L S, Lloyd S and Mazo J J 1999 *Phys. Rev. B* **60** 15398
- [12] Paauw F G, Fedorov A, Harmans C J P M and Mooij J E 2009 *Phys. Rev. Lett.* **102** 090501
- [13] Lanting T, Berkley A J, Bumble B, Bunyk P, Fung A, Johansson J, Kaul A, Kleinsasser A, Ladizinsky E, Maibaum F, Harris R, Johnson M W, Tolkacheva E and Amin M H S 2009 *Phys. Rev. B* **79** 060509(R)
- [14] Harris R, Johnson M W, Han S, Berkley A J, Johansson J, Bunyk P, Ladizinsky E, Govorkov S, Thom M C, Uchaikin S, Bumble B, Fung A, Kaul A, Kleinsasser A, Amin M H S and Averin D V 2008 *Phys. Rev. Lett.* **101** 117003
- [15] Kroger H, Smith L N and Jillie D W 1981 *Appl. Phys. Lett.* **39** 280
- [16] Zhu X B, Kemp A, Saito S and Semba K 2010 *Appl. Phys. Lett.* **97** 102503
- [17] Robertson T L, Plourde B L T, Reichardt P A, Hime T, Wu C E and Clarke J 2006 *Phys. Rev. B* **73** 174526
- [18] Kamon M, Tsuk M J and White J K 1994 *IEEE T Microw Theory* **42** 1750